Sustainable Maritime Transportation and Exploitation of Sea Resources – Rizzuto & Guedes Soares (eds)

Theoretical and experimental investigation on the total resistance of an underwater ROV remotely operating vehicle

D. Obreja & L. Domnisoru
"Dunarea de Jos" University of Galati, Galati, Romania

ABSTRACT: The present study focuses on the theoretical and experimental hull resistance analysis of an underwater ROV remotely operating vehicle, small in mass and dimensions, used for maritime and offshore operations survey at 30 m design depth. In order to evaluate the mini-ROV resistance, with and without free surface influence, both experimental and statistical methods were applied. An ellipsoidal body shape was selected, whose main dimensions were $500 \times 350 \times 250$ mm, having horizontal and vertical propeller tubes in the external shell structure, placed at both sides and ends. In the experimental tests four different immersion cases are analysed, corresponding to the speed domain 1 to 2 m/s. The 1:1 scale experimental ROV model tests were performed at the Towing Tank of the Naval Architecture Faculty, from the "Dunarea de Jos" University of Galati. The comparison between the experimental results and statistical predictions evinced the overestimation of the mini-ROV resistance based on statistical relations.

1 INTRODUCTION

The present day construction and exploitation of the maritime and offshore devices require periodic underwater survey. One of the practical solutions is the survey based on underwater ROV remotely operating vehicles (Christ & Wernli, 2007; Griffiths, 2003).

As a rule, a modern ROV has to carry out different tasks. A wide diversity of technical solutions, in terms of shape, general arrangement, propulsion system and onboard devices can be obtained (Valencia et al., 2008; Ross, 2006; Domnisoru et al., 2010).

The experimental resistance tests of the mini-ROV is carried out on a 1:1 scale built ROV model, attached to the towing tank carriage by means of a hydrodynamically-shaped support. The ROV model resistance is obtained from the difference between the total resistance of the ROV-profile support system and the resistance of the hydrodynamic profile support only. In order to point out the free surface influence on the resistance force, the experimental tests include four different immersion cases, the test speed ranging from 1 to 2 m/s. Section 3 illustrates the experimental tests performed at the Naval Architecture Faculty Towing Tank, at the "Dunarea de Jos" University of Galati, using a new Cussons Technology Ltd. measuring system (Cussons, 2009).

The study includes also under Section 4 an evaluation of the mini-ROV model resistance, based on fluid mechanics statistical relations (Blevins, 2003; Munson et al., 2004; Batchelor, 2000), applied to an ellipsoidal body shape, without the free surface influence.

The statistical values represent the comparing reference data base for the experimental test results.

2 THE MINI ROV HULL CHARACTERISTICS

In the present study the experimental resistance tests are developed for a concept of our own design of a mini-ROV model (Domnisoru et al., 2010), used for general purpose applications, whose main dimensions are shown in Table 1, and hull structural layout in Figure 1a.

The mini-ROV design has only one external watertight shell, ellipsoidal in shape. In order to obtain a compact mini-ROV design, the propulsion systems for horizontal and vertical motions are mounted symmetrically, at the sides as well as the ends, in the external shell propulsion tubes (Fig. 1a).

Table 1. The main dimensions of the mini-ROV ellipsoidal hull model.

$2a$ [mm]	500	e_1 [mm]	215
$2b$ [mm]	350	f_1 [mm]	35
$2c$ [mm]	250	e_2 [mm]	140
d [mm]	50	f_2 [mm]	35
Δ [kg]	21.3	M_{hull}[kg]	5.2
$M_{devices}$[kg]	16.2	v [Knots]	3

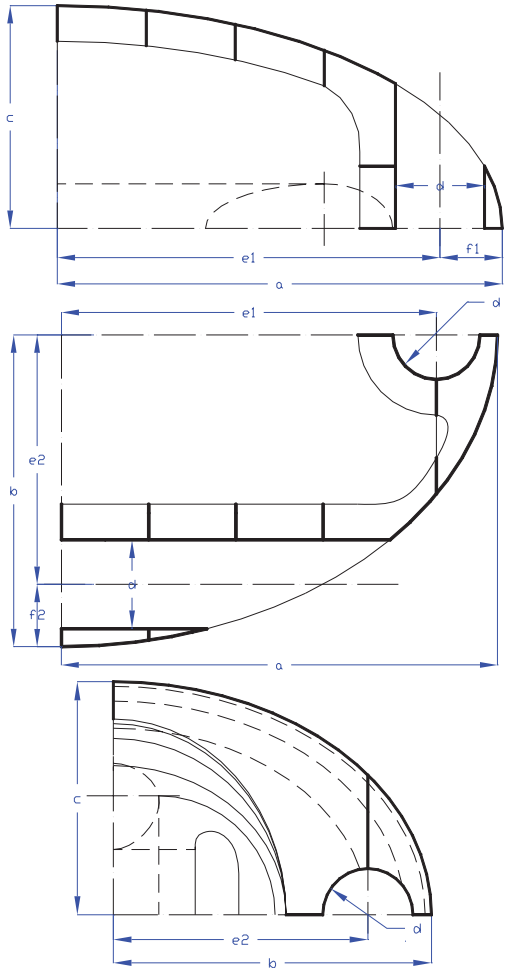

Figure 1a. The mini-ROV's ellipsoidal hull layout design model.

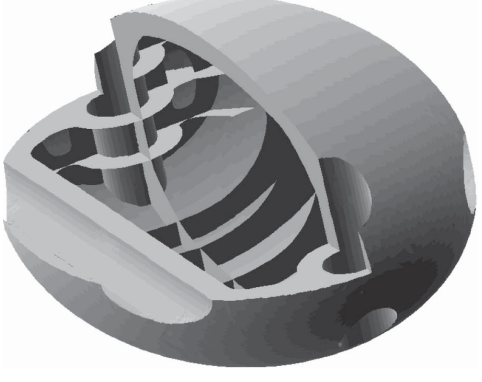

Figure 1b. The mini-ROV's ellipsoidal hull 3D CAD design model.

Figure 1b shows our own 3D CAD design concept for the experimental model of the mini-ROV.

The ROV hull model is made of composite fibreglass material (GL, 2011), with structural strengths corresponding to the design operation depth of 30 m.

The mass of the hull structure is 5.2 kg, resulting in a 16.2 kg onboard devices carrying capacity.

The design speed is 3 Knots (1.54 m/s), so that the experimental testing speeds range is set to 1÷2 m/s.

3 EXPERIMENTAL INVESTIGATION ON THE TOTAL RESISTANCE OF THE MINI-ROV

3.1 *The experimental mini-ROV model and the set-up of the towing tank test facilities*

The experimental tests used to measure the ROV model resistance in a forward motion were carried out in the Towing Tank of the Faculty of Naval Architecture of the "Dunarea de Jos" University of Galati (Fig. 2).

The Towing Tank, $45 \times 4 \times 3$ meters in size, is fitted with an automatic carriage able to tow experimental models at a maximum speed of 4 m/s, built by the British Company Cussons Technology, operating since 2009 (Cussons, 2009).

In order to measure the resistance in forward motion, the forward motion resistance dynamometer R35 was used, the measuring range being up to 200 N and the measuring error 0.2%. By applying the standard procedure, the calibration constant of the dynamometer was determined (1.05268 V/N).

The ROV experimental model was built at a 1:1 scale on the basis of the shape plan generated by the "Dunarea de Jos" University of Galati. In order to determine the resistance in forward motion, the submerged ROV model was coupled to the carriage by means of a support with a symmetrical hydrodynamic profile, of segment type

Figure 2. Towing Tank of the "Dunarea de Jos" University of Galati, Naval Architecture Faculty.

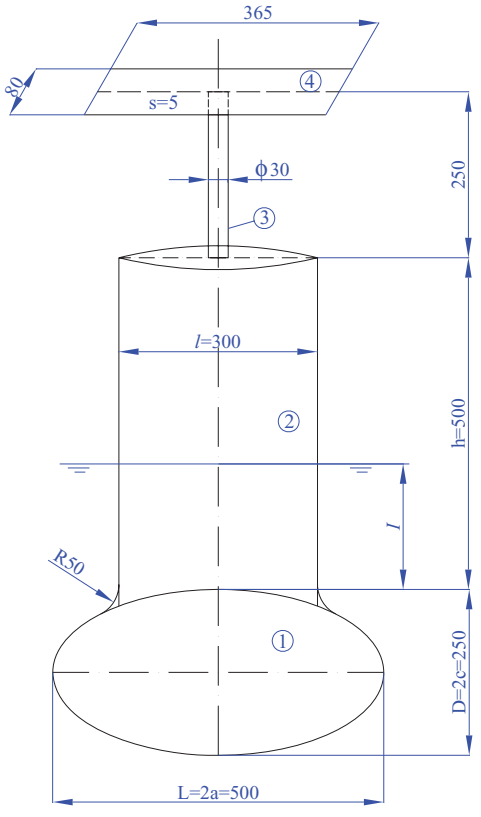

Figure 3. The mini-ROV-hydrodynamic profile support system components: 1- the ROV hull model; 2- the hydrodynamic profile support; 3-beam support; 4-plate support mounted on the resistance dynamometer.

(Fig. 3), generating its own waves of medium amplitudes. The geometric characteristics of the hydrodynamic profile are shown in Table 2.

Measurements were performed both for the forward motion resistance of the system made up of the ROV and the hydrodynamic support, and of the hydrodynamic support by itself. In the hypothesis of overlapping effects, the forward motion resistance of the ROV model is the difference between the resistance of the ROV-hydrodynamic system and the hydrodynamic support resistance.

The automatic system of experimental data acquisition and analysis used for processing the results of experimental tests was developed by the Cussons company. The electric signals transmitted by the forward motion resistance translator were automatically acquired and transformed into physical dimensions by applying the calibration constant. The sampling time step was 0.1 s, and the sample number depended on the carriage speed (390 samples at the minimum speed 1 m/s and 220 samples at the maximum speed of 2 m/s).

Table 2. Characteristics of the hydrodynamic support.

Profile thickness, $t = 0.036$ m	Aspect ratio, $h/l = 1.667$
Profile length, $l = 0.300$ m	Relative thickness, $t/l = 0.12$

The average values of the experimental results were calculated for the stationary flow range. The measurement error of the forward motion resistance tests was about 2%.

The serial of experimental tests included sets of trials for 4 different immersions of the hydrodynamic support (0.05 m, 0.35 m, 0.45 m, 0.55 m) in order to determine the influence of the free surface upon the forward motion resistance. Also, keeping into account the designed value of the speed, the evolution of the forward motion resistance was analysed within a range between 1 m/s and 2 m/s, at a step of 0.25 m/s.

3.2 *Experimental resistance tests on the hydrodynamic profile support*

The experimental results of forward motion resistance tests of the hydrodynamic profile support are shown in Table 3. Figure 4 illustrates the diagram of the forward motion resistance R_{Ts} function of the speed v, for the four immersion cases analysed.

Generally speaking, the forward motion resistance of the hydrodynamic support increases with speed. Only in the case of minimal immersion, $I = 0.05$ m, the forward motion resistance does not significantly depend on speed within the analysed range.

Figure 5 shows the diagram of the forward motion resistance of the hydrodynamic support, R_{tS} in relation to immersion I, for constant speeds. Naturally, there is an increase of the forward motion resistance of the hydrodynamic support with the immersion depth.

Figures 6a, b, c show the flow around the hydro-dynamic support at maximum immersion $I = 0.55$ m, at speeds of 1 m/s, 1.5 m/s and 2 m/s respectively. The Figures 6 analysis leads to the following observations:

- the segment profile attack board generates its own wave of moderate height;
- at the bow of the flight board there is increased wake at the speed of 1 m/s, with vortices and broken waves;
- due to the segment profile flight board, the wake width significantly decreases with the increase of the speed.

Figures 7a, b, c show the flow around the hydrodynamic support at the speed of 1.5 m/s, at

Table 3. Resistance of the hydrodynamic support, R_{tS} [N].

Immersion I [m]	Speed, v [m/s]				
	1	1.25	1.5	1.75	2
0.05	0.57	0.60	0.53	0.56	0.68
0.35	1.54	1.91	1.97	2.18	2.44
0.45	1.99	2.24	2.43	2.64	2.90
0.55	2.07	2.54	2.79	3.01	3.55

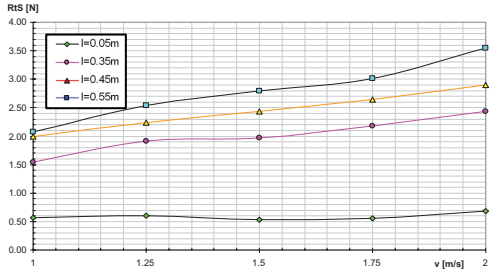

Figure 4. Resistance of the hydrodynamic support function of speed, at constant immersion (0.05, 0.35, 0.45, 0.55 m).

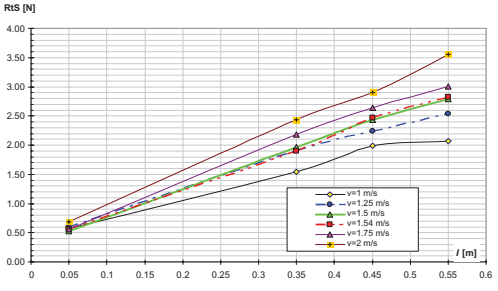

Figure 5. Resistance of the hydrodynamic support function of immersion, at constant speed (1, 1.25, 1.5, 1.75, 2 m/s).

Figure 6a. Hydrodynamic support, immersion $I = 0.55$ m and speed $v = 1$ m/s.

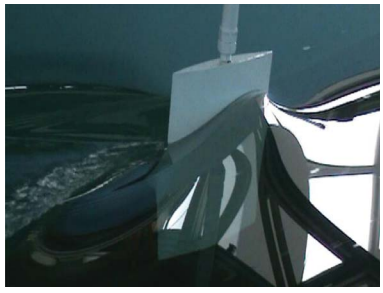

Figure 6b. Hydrodynamic support, immersion $I = 0.55$ m and speed $v = 1.5$ m/s.

Figure 6c. Hydrodynamic support, immersion $I = 0.55$ m and speed $v = 2$ m/s.

Figure 7a. Hydrodynamic support, immersion $I = 0.05$ m and speed $v = 1.5$ m/s.

Figure 7b. Hydrodynamic support, immersion $I = 0.35$ m and speed $v = 1.5$ m/s.

Figure 7c. Hydrodynamic support, immersion $I = 0.55$ m and speed $v = 1.5$ m/s.

immersions of 0.05 m, 0.35 m and 0.55 m. Except for the minimum immersion case, no noticeable differences occur in the hydrodynamic spectre of the flow around the hydrodynamic profile. The wake field contains vortices and broken waves.

3.3 *Experimental resistance tests on the mini-ROV hull coupled to the hydrodynamic profile support*

The second stage of the experimental tests contained the measurements of the forward motion resistance for the system consisting of the ROV and the hydrodynamic profile support, for the same range of speeds and immersions.

The experimental results are shown in Table 4. Figure 8 shows the diagram of the forward motion resistance R_{tA} function of the speed v, for the 4 immersions I tested, and Figure 9 shows the diagram of the forward motion resistance of the ROV- hydrodynamic support, R_{tA} in relation to the immersion I, at the 5 speeds under consideration.

The following observations were derived from the experimental data:

– the forward motion resistance of the ROV-hydrodynamic support system increases with speed, except for the minimum immersion $I = 0.05$ m, where there is a significant decrease of the forward motion resistance starting from speeds higher than 1.5 m/s (Fig. 8), which was confirmed by repeated tests;
– the forward motion resistance of the ROV-hydrodynamic support system decreases at minimum immersion ($I = 0.05$ m) for speeds under 1.5 m/s, which may be explained by the considerable calming of the flow's hydrodynamic spectre within this speed range, as seen in Figures 10a, b, c;

Table 4. Resistance of the ROV-hydrodynamic support, R_{tA}[N].

Immersion I [m]	Speed, v [m/s]				
	1	1.25	1.5	1.75	2
0.05	21.19	34.23	43.87	36.39	29.65
0.35	8.07	12.73	16.44	20.47	25.44
0.45	7.78	11.73	16.36	20.28	25.34
0.55	7.77	11.37	16.21	20.19	24.44

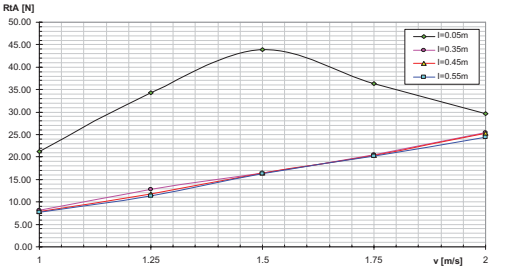

Figure 8. Resistance of the ROV-hydrodynamic support system function of speed, at constant immersion (0.05, 0.35, 0.45, 0.55 m).

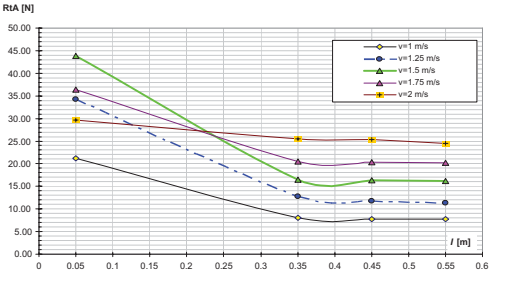

Figure 9. Resistance of the ROV-hydrodynamic support system function of immersion, at constant speed (1, 1.25, 1.5, 1.75, 2 m/s).

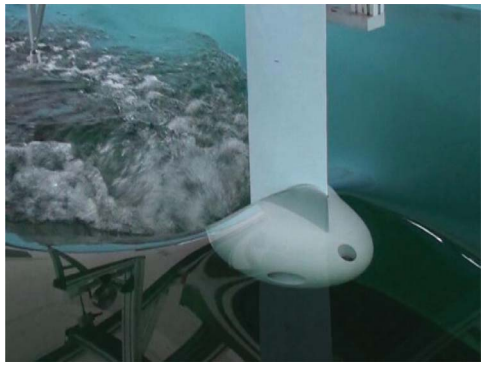

Figure 10a. ROV-hydrodynamic support system, immersion $I = 0.05$ m and speed $v = 1.5$ m/s.

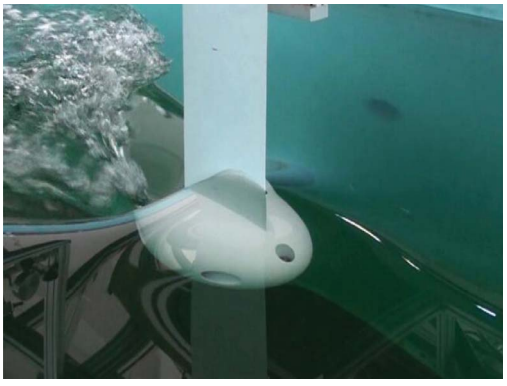

Figure 10b. ROV-hydrodynamic support system, immersion $I = 0.05$ m and speed $v = 1.75$ m/s.

Figure 10c. ROV-hydrodynamic support system, immersion $I = 0.05$ m and speed $v = 2$ m/s.

- the values of the forward motion resistance at the minimum immersion $I = 0.05$ m are much higher than for the other immersions tested, due to the negative effect of the free surface;
- in the case of the immersions $I = 0.45$ m and $I = 0.55$ m there are very small differences between the values of the forward motion resistance of the ROV- hydrodynamic support system; the increase of the forward motion resistance due to the increased immersion of the ROV- hydrodynamic support system is practically compensated for by the decrease in the forward motion resistance resulting from the decreased effect of the free surface.

Similarly, Figures 11a, b, c illustrate the flow around the ROV- hydrodynamic support system,

Figure 11a. ROV-hydrodynamic support system, immersion $I = 0.55$ m and speed $v = 1$ m/s.

Figure 11b. ROV-hydrodynamic support system, immersion $I = 0.55$ m and speed $v = 1.5$ m/s.

Figure 11c. ROV-hydrodynamic support system, immersion $I = 0.55$ m and speed $v = 2$ m/s.

at the maximum immersion $I = 0.55$ m, for speeds equal to 1 m/s, 1.5 m/s and 2 m/s, respectively.

Figures 12a, b, c show the flow around the ROV- hydrodynamic support system, at the speed of 1.5 m/s, for the immersions 0.05 m, 0.35 m and 0.55 m.

The analysis of the hydrodynamic spectres of the ROV- hydrodynamic support system allows the following observations:

– the height of the own wave is above the one in the hydrodynamic support tests, and the length and height of the stern waves increases with the current speed;
– the wake width significantly decreases when the current speed increases;
– at the minimum immersion $I = 0.05$ m, the wake of the ROV- hydrodynamic support system is more noticeable than in the case of the hydrodynamic support alone, generating broken waves and strong vortices; the influence of the ROV hull, located close to the free surface, on the aspect of hydrodynamic flow is very important;
– for the other cases of immersion, there are no noticeable differences in the hydrodynamic spectre of the flow at the same speed; a strong uneven wake is generated at bow, with vortices and broken waves at the ends of the wake field, similar to the wake created by the hydrodynamic support.

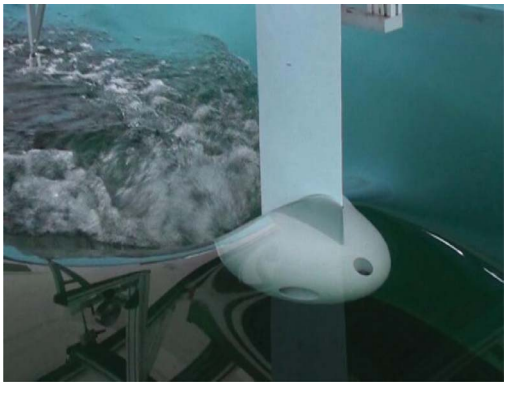

Figure 12a. ROV-hydrodynamic support system, immersion $I = 0.05$ m and speed $v = 1.5$ m/s.

Figure 12b. ROV-hydrodynamic support system, immersion $I = 0.35$ m and speed $v = 1.5$ m/s.

Figure 12c. ROV-hydrodynamic support system, immersion $I = 0.55$ m and speed $v = 1.5$ m/s.

3.4 *The mini-ROV resistance analysis*

Based on the comparative analysis between the eigen wave patterns generated at the maximum immersion by the hydrodynamic support (Figs. 6a, b, c) and by the mini-ROV hull and hydrodynamic support system (Figs. 11a, b, c), it results that for the tested speed domain the influence of the immerged hull is very reduced in compare to the hydrodynamic support. These justifies the use of the linear hypothesis, so that the forward motion resistance of the ROV model is determined as the difference between the resistance of the ROV—hydrodynamic support system and the hydrodynamic support resistance:

$$R_{trOV} = R_{tA} - R_{tS} \tag{1}$$

The results of the calculations are provided in Table 5. Figure 13 shows the diagram of the forward motion resistance R_{tROV} versus speed v, at the 4 immersions I tested, while Figure 14 shows the diagram of the ROV forward motion resistance, R_{tROV} in relation to the immersion I, for the 5 speed cases.

Result analysis leads to the following observations:

– the ROV forward motion resistance increases with speed, except for the minimum immersion

I = 0.05 m case, where a significant decrease of the forward motion resistance is seen at speeds over 1.5 m/s (Fig. 13);
– the values of the forward motion resistance at the minimum immersion I = 0.05 m are much higher than at the other immersions tested, which proves the negative effect of the free surface;
– in the cases of immersions ranging from 0.45 m to 0.55 m, the influence of the free surface decreases, yet maximum reductions of about 7% in the forward motion resistance are noticed with the increase of immersion, within the speed range analysed.

Considering by approximation that the variation diagram of the ROV forward motion resistance is the diagram corresponding to the maximum immersion, I = 0.55 m, the actual towing power P_{EROV} at v speed was calculated by means of the relation (see Table 6):

$$R_{EROV} = R_{tROV} \cdot v \tag{2}$$

Table 5. ROV resistance, R_{tROV} [N].

Immersion I [m]	Speed, v [m/s]				
	1	1.25	1.5	1.75	2
0.05	20.62	33.63	43.34	35.83	28.97
0.35	6.53	10.82	14.47	18.29	23.0
0.45	5.79	9.49	13.93	17.64	22.44
0.55	5.70	8.83	13.42	17.18	20.89

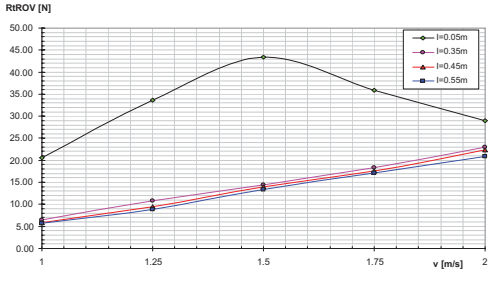

Figure 13. ROV resistance function of speed, at constant immersion (0.05, 0.35, 0.45, 0.55 m).

Table 6. ROV resistance and effective power versus speed.

v [m/s]	1	1.25	1.5	1.75	2
R_{tROV} [N]	5.70	8.83	13.42	17.18	20.89
P_{EROV} [W]	5.70	11.04	20.13	30.07	41.78

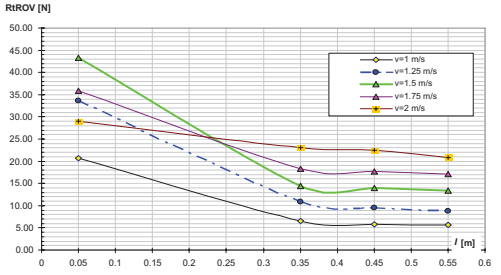

Figure 14. ROV resistance depending of the immersion, at constant speed (1, 1.25, 1.5, 1.75, 2 m/s).

4 THE MINI-ROV DRAG FORCE PREDICTION BASED ON STATISTICAL RELATIONS

In order to obtain preliminary reference values for the towing tank experimental data, this section focuses on the mini-ROV hull model drag force and power evaluation based on fluid mechanics statistical relations (Blevins, 2003; Munson et al., 2004).

The statistical approach for the min-ROV drag force and power evaluation is applied according to the following hypothesis:

– the immerse ellipsoidal body has the same dimensions and speed as the ROV vehicle (Table 1);
– the ellipsoidal shape is smooth and complete, without taking into account the ROV horizontal and vertical propulsion tubes (d = 0);
– the free surface influence is neglected, considering the immersion at full operation depth 30 m.

The statistical drag force and power are obtained with Equation 3, with C_x statistical coefficient from Table 7 (Blevins, 2003; Munson et al., 2004).

Table 8 shows the resulting statistical drag force and power values for the min-ROV ellipsoidal hull model, without propulsion tubes and free surface influence.

$$R_{tROV\,st} = C_x \rho_a \frac{v^2}{2} A_E [\mathrm{N}];\ P_{EROV\,st} = R_{tROV\,st}\, v [\mathrm{W}]$$
$$C_x = f(R_{eE});\ R_{eE} = \frac{vL}{\upsilon};\ \upsilon = \frac{\mu}{\rho_a};\ L = 2a;\ A_E = \pi b c \tag{3}$$

where: $R_{tROV\,st}$ [N], $P_{EROV\,st}$ [W] are the full immerse ellipsoidal hull statistical drag force and power; C_x is the non-dimensional drag force coefficient; R_{eE} is the Reynolds number; ρ_a = 998.2 kg/m^3, μ = 1.002 10^{-3} Pa · s, υ = 1.004 10^{-6} m^2/s are the water density, dynamic and cinematic viscosity, for

Table 7. Statistic drag force non-dimensional coefficient for full immerse ellipsoidal body (Blevins, 2003; Munson et al., 2004).

R_{eE}	$\log_{10}(R_{eE})$	C_x	R_{eE}	$\log_{10}(R_{eE})$	C_x
$1.00\ 10^1$	1.00	8.00	$1.00\ 10^5$	5.00	0.47
$1.00\ 10^2$	2.00	1.00	$5.00\ 10^5$	5.70	0.29
$5.00\ 10^2$	2.70	0.50	$1.00\ 10^6$	6.00	0.15
$1.00\ 10^3$	3.00	0.47	$1.00\ 10^7$	7.00	0.10

Table 8. ROV resistance and effective power of the immerse ellipsoidal ROV hull, based on statistic values for the C_x drag force coefficient.

v[m/s]	R_{eE}	$\log_{10}(R_{eE})$	C_x	R_{tROVst} [N]	P_{EROVst} [W]
1.00	4.98E + 05	5.70	0.29	9.79	9.79
1.25	6.23E + 05	5.79	0.24	12.97	16.22
1.50	7.47E + 05	5.87	0.21	15.95	23.92
1.75	8.72E + 05	5.94	0.18	18.56	32.48
2.00	9.96E + 05	6.00	0.15	20.68	41.36

t = 20°C reference tests temperature; v = 1÷2 m/s is the model speed testing range; L = 0.500 m is the model reference length; A_E = 0.06872234 [m²] is the frontal reference area of the immerse ellipsoidal body; a, b, c [m] are the hull model main dimensions (Table 1).

5 CONCLUSIONS

Based on the experimental tests data in Section 3 and the statistic values in Section 4, the following conclusions were drawn for the mini-ROV resistance analysis:

1. The mini-ROV resistance, based on experimental tests, increases with speed for all immersions, except for the minimum immersion case when a significant decrease of the resistance is recorded for speeds higher than 1.5 m/s (Table 5, Fig. 13).
2. The decrease of the resistance recorded for the minimum immersion may be accounted for on the basis of a flow around the hull without vortices or its own braking waves, for speeds higher than 1.5 m/s (Figs. 10a, b, c).
3. The negative effect of the free surface on the mini-ROV hull resistance, determined by experimental tests, decreases when the immersion of the ROV-hydrodynamic profile system increases. The free surface effect explains the highest ROV resistance for the minimum immersion case (I = 0.05 m).

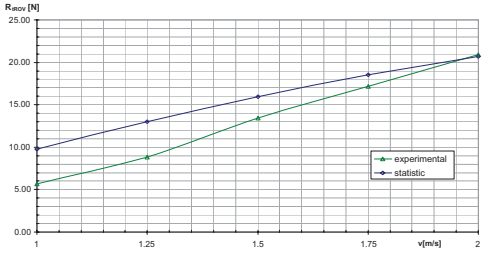

Figure 15. Statistical and experimental diagrams of the mini-ROV resistance, at maximum immersion.

4. The mini-ROV resistance based on experimental tests (Table 6) is 14.13 N for the design speed of 1.54 m/s (3 Knots). The effective power calculated at design speed is 21.76 W.
5. The mini-ROV resistance estimations, based on fluid mechanical statistical relations of an ellipsoidal immerse body (Blevins, 2003; Munson et al., 2004), without propeller tubes and free surface influence (Table 8) is 16.43 N for the design speed of 1.54 m/s (3 Knots). The statistically effective power at design speed is 25.35 W.
6. Comparing the experimental results and the statistical predictions (Fig. 15) results in the fact that the mini-ROV resistance based on statistical relations is overestimated by 16.28% for the reference design speed of 1.54 m/s (3 Knots).
7. For 2 m/s speed the ROV experimental and statistical values are almost de same, but the resistance versus speed curves slope are different (Fig. 15).
8. The extreme eigen wave pattern generated at the hydrodynamic support stern in low speed cases induces a significant increase of the support initial resistance (Figs. 6 & 11). Based on the superposition hypothesis, it results that the ROV hull resistance has a significant decrease for lower speed cases. These results are justifying the high differences between experimental and statistical resistance values for the lower speed domain (Fig. 15).

ACKNOWLEDGEMENTS

The work has been performed within the scope of the projects for mini-ROV submerged vehicles design and fluid flow analysis on hydrodynamic profiles financed by the Romanian Education and Research Ministry, under contracts CNMP-PNII-P4/3401/12-116/2008-2011 and CNCSIS PNII-ID-790/2008-2011.

REFERENCES

Batchelor, G. 2000. *An introduction to fluid dynamics*, Cambridge: Cambridge University Press.

Blevins, Robert, D. 2003. *Applied fluid dynamics handbook*. Malabar, Florida: Krieger Publishing Company.

Christ Robert, D., Wernli, Sr. & Robert, L. 2007. *The ROV manual. A user guide to observation-class remotely operated vehicles.* Oxford: Butterworth Heinemann.

Cussons. 2009. Marine hydrodynamic research. Cussons Technology Ltd. Manchester.

Domnisoru, L., Dumitru, D. & Mocanu, C. 2010. *Initial structural design of an submerged vehicle, made of composite materials*. Galati: Galati University Press.

GL. 2011. Germanischer Lloyd's Rules. Non-metallic materials. Remotely operated underwater vehicles. Hamburg.

Griffiths, G. 2003. *Technology and applications of autonomous underwater vehicles*. London: Taylor & Francis.

Munson, Bruce, R., Young, Donald, F. Young & Okishi, Theodore, H. 2004. *Fundamentals of fluid mechanics*. New York: John Wiley & Sons Publications.

Ross, C. 2006. *A conceptual design of an underwater vehicle.* Ocean Engineering, Vol. 33, pp. 2087–2104, 2006.

Valencia, R.A., Ramirez, J.A., Gutierrez, L.B. & Garcia, M.J. 2008. Modelling and simulation of an underwater remotely operated vehicle for surveillance and inspection of port facilities using CFD tools. Proceedings of the ASME 27th International Conference OMAE 2008, Estoril.